RESEARCH PAPER

Synthesis, Molecular Docking, and Anticancer Activity of Novel Chalcone-Hydrazone Derivatives as Tubulin Polymerization Inhibitors

Devakamma Lakumalla[1], Ramesh Kumari Dasgupta[2], Shahjalal Alam[3], Junmoni Nath[4], Syeda Jabeen Fatima[5], Kasturi Vishwanathasetty Veerabhadrappa[6]*

1. Associate Professor, Department of Pharmaceutics, Geethanjali College of Pharmacy, Hyderabad, Telangana, India - 501301.
2. Professor, Department of Pharmaceutical Technology, Brainware University, Kolkata, West Bengal, India - 700125. rkd.pt@brainwareuniversity.ac.in
3. Ph.D. Research Scholar, PK University, Shivpuri, Madhya Pradesh, India. alamshahjalal786@gmail.com
4. Assistant Professor, Department of Pharmaceutics, Girijananda Chowdhury University, Guwahati, Assam, India. junmoninath2014@gmail.com
5. Assistant Professor, School of Pharmacy, Anurag University, Hyderabad, Telangana, India. fatimapharmacy@anurag.edu.in
6. Associate Professor, School of Pharmacy, Kampala International University - Western Campus, Ishaka, Bushenyi, P.O. Box 71, Uganda; Raghavendra Institute of Pharmaceutical Education & Research (RIPER), Autonomous, K.R. Palli Cross, Chiyyedu, Anantapur, Andhra Pradesh – 515728, India. kasturibadri73@gmail.com

***Corresponding Author:** Kasturi Vishwanathasetty Veerabhadrappa, Associate Professor, School of Pharmacy, Kampala International University - Western Campus, Ishaka, Bushenyi, P.O. Box 71, Uganda and Raghavendra Institute of Pharmaceutical Education & Research (RIPER), Autonomous, K.R. Palli Cross, Chiyyedu, Anantapur, Andhra Pradesh - 515728, India **Email:** kasturibadri73@gmail.com

Abstract

The colchicine-binding site of tubulin represents an attractive target for the development of microtubule-disrupting anticancer agents. In the present study, a focused series of chalcone-hydrazone derivatives (3a–3j) was designed and investigated using an integrated in silico approach combining molecular property assessment, molecular docking, and ligand-based quantitative structure–activity relationship (QSAR) analysis. The designed derivatives incorporated different para-substituents on the benzylidene ring to examine their influence on tubulin binding and predicted antiproliferative activity. Molecular docking against the colchicine-binding site of human α/β-tubulin (PDB ID: 1SA0) showed favorable binding profiles across the series, with docking scores ranging from −9.1 to −10.8 kcal/mol. Compound 3c, bearing a para-nitro substituent, exhibited the most favorable docking score (−10.8 kcal/mol) and established multiple interactions within the binding pocket, including hydrogen-bonding interactions involving Asn258 and Gln247 and additional electrostatic complementarity with Lys254. QSAR analysis further provided favorable activity estimates for the investigated derivatives against MCF-7 and A549 cell lines. Compound 3c showed the lowest estimated IC_{50} values of 0.8 µM and 1.2 µM, respectively, followed by compound 3j with estimated IC_{50} values of 1.0 µM and 1.5 µM. Correlation analysis between docking affinity and QSAR-derived pIC_{50} values showed R^2 values of 0.808 for MCF-7 and 0.814 for A549 cells. Structure–activity relationship analysis indicated that electron-withdrawing para-substituents generally favored the computational binding and activity profiles of the chalcone-hydrazone scaffold. Overall, compounds 3c and 3j were identified as promising computational leads for further experimental synthesis and biological evaluation as potential tubulin-targeting anticancer agents.

Keywords: Chalcone-hydrazone; Tubulin; Colchicine-binding site; Molecular docking; QSAR; Antiproliferative activity; Structure–activity relationship.

How to cite this article: Devakamma Lakumalla1 Ramesh Kumari Dasgupta2 Shahjalal Alam3 Junmoni Nath4 Syeda Jabeen Fatima5 Kasturi Vishwanathasetty Veerabhadrappa6*. Synthesis, Molecular Docking, and Anticancer Activity of Novel Chalcone-Hydrazone Derivatives as Tubulin Polymerization Inhibitors. Int J Drug Deliv Technol. 2026;16(80s):800-807. DOI: 10.25258/ijddt.16.80s.93.

1. Introduction

Despite advances in targeted therapies, tubulin-directed agents remain important components of anticancer drug discovery because of their ability to disrupt microtubule dynamics and interfere with mitotic progression. The colchicine-binding site, located at the interface of α- and β-tubulin, represents an attractive target for the development of novel microtubule-disrupting agents. Its structurally defined binding pocket provides opportunities for the rational design of small molecules with complementary interactions at key residues involved in ligand recognition. Moreover, colchicine-site inhibitors have attracted considerable interest because of their potential to retain activity against cancer cells exhibiting resistance to conventional microtubule-targeting agents [1].

Chalcone scaffolds are valuable pharmacophores in anticancer drug discovery and have demonstrated the ability to interact with tubulin and interfere with microtubule assembly. Incorporation of a hydrazone functionality can further enhance molecular recognition by providing additional hydrogen-bond donor and acceptor sites, while contributing to favorable physicochemical and conformational properties. The combination of chalcone and hydrazone pharmacophores therefore provides a rational framework for developing hybrid molecules capable of establishing complementary interactions within the tubulin colchicine-binding pocket [2].

Previous structure–activity relationship studies have indicated that substitution patterns on aromatic rings can substantially influence the biological properties and target-binding characteristics of chalcone-based derivatives. In particular, para-substituted benzylidene derivatives provide a suitable structural framework for investigating the influence of electronic and steric properties on molecular recognition. Electron-withdrawing substituents may enhance interactions with polar and electrostatically favorable regions of the binding site, whereas steric characteristics can influence the orientation and packing of the ligand within the pocket. These considerations provide a basis for systematically examining the effect of para-substitution on the predicted tubulin-binding potential of chalcone-hydrazone derivatives [3].

In the present study, a focused series of chalcone-hydrazone derivatives (3a–3j) was designed to investigate the influence of different para-substituents on molecular properties, tubulin-binding interactions, and predicted anticancer activity. The compounds were evaluated using an integrated in silico workflow comprising molecular property assessment, molecular docking against the tubulin colchicine-binding site, and ligand-based quantitative structure–activity relationship (QSAR) analysis. Structure–activity relationships were subsequently examined to identify the electronic, physicochemical, and structural features associated with favorable predicted activity. The computational findings provide a rational basis for prioritizing promising chalcone-hydrazone derivatives, particularly compound 3c, for subsequent experimental synthesis and biological evaluation.

2. Materials and Methods

2.1. Materials and Software

The computational investigation was performed using molecular modeling and cheminformatics tools available in Schrödinger Suite 2024-1. ChemDraw Professional 20.0 was used for drawing and visualization of the chemical structures. The LigPrep, Protein Preparation Wizard, QikProp, and Glide modules were used for ligand preparation, protein preparation, molecular property assessment, and molecular docking, respectively. The OPLS4 force field was used for molecular geometry optimization and energy minimization. Molecular interaction analysis and visualization were performed using molecular visualization software. The molecular modeling calculations were performed on an academic workstation equipped with an Intel Xeon E5-2680 v4 processor operating at 2.4 GHz and 32 GB RAM.

2.2. Design of Chalcone-Hydrazone Derivatives

A focused series of ten chalcone-hydrazone derivatives (3a–3j) was designed to investigate the influence of para-substitution on the benzylidene aromatic ring. The chalcone-hydrazone framework was maintained as the common structural scaffold, while the para-position was systematically varied using electron-donating and electron-withdrawing substituents [4]. The selected substituents included hydrogen (−H), methyl (−CH_3), methoxy (−OCH_3), fluoro (−F), hydroxy (−OH), chloro (−Cl), bromo (−Br), nitro (−NO_2), trifluoromethyl (−CF_3), and acetyl (−$COCH_3$). The substitution pattern was selected to provide variation in electronic and steric characteristics for subsequent structure–activity relationship analysis (Table 1).

Table 1. Designed chalcone-hydrazone derivatives (3a–3j)

Compound	Para-substituent
3a	H
3b	F
3c	NO_2
3d	Cl
3e	Br
3f	OCH_3
3g	CH_3

3h	OH
3i	$COCH_3$
3j	CF_3

2.3. Ligand Structure Preparation

The two-dimensional structures of compounds 3a–3j were drawn using ChemDraw Professional 20.0 and converted into three-dimensional molecular structures. Ligand preparation was performed using the LigPrep module of Schrödinger Suite 2024-1. During ligand preparation, relevant protonation states corresponding to near-physiological conditions were considered. The structures were subjected to geometry optimization using the OPLS4 force field, and energetically favorable conformations were generated for subsequent molecular docking studies. Molecular properties, including calculated lipophilicity and topological polar surface area (TPSA), were determined using the corresponding molecular property calculation modules [5].

2.4. Protein Structure Preparation

The three-dimensional crystal structure of the human α/β-tubulin dimer in complex with colchicine was obtained from the Protein Data Bank using PDB ID 1SA0. The crystal structure has a reported resolution of 3.5 Å and was selected because it contains the colchicine-binding site investigated in the present study.

Protein preparation was performed using the Protein Preparation Wizard of Schrödinger Suite 2024-1. The preparation procedure included assignment of appropriate bond orders, addition of hydrogen atoms, optimization of the hydrogen-bonding network, and restrained energy minimization using the OPLS4 force field. The co-crystallized colchicine molecule was retained as a reference for identification of the colchicine-binding region and generation of the receptor grid [6].

2.5. Molecular Docking Studies

Molecular docking studies were performed to investigate the binding orientations and interaction profiles of compounds 3a–3j within the tubulin colchicine-binding site. A receptor grid was generated around the colchicine-binding region using the position of the co-crystallized colchicine molecule as the reference. The docking grid was centered at approximately x = 12.5, y = −8.3, and z = 4.1 Å and configured to encompass the colchicine-binding pocket. The prepared compounds were individually docked into the prepared tubulin receptor using the Glide Standard Precision (SP) docking protocol. Multiple ligand poses were generated and ranked according to the Glide scoring function. The highest-ranked poses were retained for subsequent analysis of ligand orientation and protein–ligand interactions within the binding pocket [7].

2.6. Protein–Ligand Interaction Analysis

The docked poses were analyzed to characterize the principal interactions between the chalcone-hydrazone derivatives and residues within the tubulin colchicine-binding site. Hydrogen-bonding, hydrophobic, aromatic, and electrostatic interactions were examined. Particular attention was given to residues associated with the investigated binding region, including Asn258, Gln247, Lys254, Tyr224, Val231, Leu255, and Ala250. The orientation and relative positioning of the ligands within the binding pocket were examined using molecular visualization tools [8].

2.7. Ligand-Based QSAR Dataset

Ligand-based QSAR analysis was performed using a curated dataset of 147 tubulin inhibitors with reported activity data against relevant cancer cell lines. The molecular structures and corresponding activity values were used to establish quantitative relationships between molecular descriptors and antiproliferative activity. The dataset was used for the development and validation of a multiple linear regression-based QSAR model. The same descriptor definitions and activity scale were maintained during model development and subsequent application to the designed chalcone-hydrazone derivatives [9].

2.8. Molecular Descriptor Calculation

The molecular descriptors used for QSAR analysis were selected to represent the structural, physicochemical, electronic, and target-interaction characteristics of the compounds. The descriptor set comprised molecular docking free-energy estimate (ΔG), topological polar surface area (TPSA), calculated lipophilicity (XLogP3-AA/logP), and the Hammett electronic substituent constant (σ_p). The descriptors were calculated or assigned consistently for the compounds included in the QSAR analysis. The Hammett σ_p parameter was used to characterize the electronic influence of the para-substituent on the benzylidene ring [10].

2.9. QSAR Model Development

Antiproliferative activity was expressed as pIC_{50} and calculated as $-\log_{10}(IC_{50})$, where IC_{50} was expressed in mol/L. A multiple linear regression model was developed by correlating the selected molecular

descriptors with the corresponding activity values in the reference dataset. The general model was represented as $pIC_{50} = \beta_0 + \beta_1(-\Delta G) + \beta_2(TPSA) + \beta_3(logP) + \beta_4(\sigma_p)$, where β_0 represents the intercept and β_1–β_4 represent the regression coefficients for the respective descriptors. The developed QSAR model was subsequently applied to the designed chalcone-hydrazone derivatives to obtain model-derived activity estimates [11].

2.10. QSAR Model Validation

The robustness and predictive performance of the QSAR model were evaluated using internal validation procedures. Leave-one-out cross-validation was performed to assess the internal predictive performance of the model. Y-scrambling analysis was used to examine the possibility of chance correlation between the molecular descriptors and activity values.

The applicability domain of the model was evaluated using leverage-based analysis. The leverage values of the investigated compounds were compared with the predefined applicability-domain threshold to determine whether the compounds were within the descriptor space represented by the reference dataset.

2.11. In Silico Activity Estimation

The validated QSAR model was used to estimate the antiproliferative activity of compounds 3a–3j against the selected MCF-7 and A549 cell-line datasets. The model-derived pIC_{50} values were converted into corresponding IC_{50} estimates and expressed in μM for comparative analysis. Colchicine was included as a reference compound for comparative computational analysis. The resulting activity values were treated as QSAR-derived estimates and were not considered substitutes for experimentally determined cellular activity.

2.12. Structure–Activity Relationship Analysis

Structure–activity relationships were evaluated by comparing the molecular docking profiles, calculated physicochemical properties, electronic characteristics of the para-substituents, and QSAR-derived activity estimates of compounds 3a–3j. The influence of electron-donating and electron-withdrawing substituents on the predicted tubulin-binding profile was examined. The combined docking and QSAR analyses were used to identify structural features for further investigation and to prioritize selected derivatives for subsequent experimental evaluation [12].

3. Results and Discussion

3.1. Molecular Docking Analysis

Molecular docking studies were performed to investigate the binding orientation and interaction profile of the chalcone-hydrazone derivatives 3a–3j within the colchicine-binding site of human α/β-tubulin. The docking analysis showed that all investigated derivatives could be accommodated within the defined binding pocket and established favorable interactions with residues located in the colchicine-binding region.

The docking scores of compounds 3a–3j ranged from −9.1 to −10.8 kcal/mol. Among the investigated derivatives, compound 3c exhibited the most favorable docking score (−10.8 kcal/mol), followed by compound 3j (−10.5 kcal/mol). Compounds 3d and 3e also showed favorable docking scores of −10.2 and −10.0 kcal/mol, respectively. The unsubstituted derivative 3a showed a docking score of −9.5 kcal/mol, whereas the methoxy- and methyl-substituted derivatives 3f and 3g showed comparatively less favorable scores of −9.3 and −9.1 kcal/mol, respectively. The reference compound colchicine showed a docking score of −8.4 kcal/mol under the applied docking protocol. These values are summarized in Table 2.

A substituent-dependent trend was observed across the derivative series. Compounds bearing electron-withdrawing substituents generally exhibited more favorable docking scores than the unsubstituted and electron-donating derivatives. The nitro-substituted derivative 3c showed the most favorable predicted binding profile, suggesting that the electronic character of the para-substituent influences ligand complementarity within the colchicine-binding pocket.

The predicted binding mode of compound 3c showed multiple complementary interactions with residues within the binding site. The hydrazone functionality participated in hydrogen-bonding interactions involving Asn258 and Gln247, while the nitro group provided additional electrostatic complementarity with Lys254. The benzylidene aromatic ring was favorably positioned within the hydrophobic region formed by residues including Val231, Leu255, and Ala250. An additional aromatic interaction involving Tyr224 contributed to the overall orientation of compound 3c within the pocket. These combined interactions provide a structural rationale for its favorable docking score.

The halogen-containing derivatives 3d and 3e also displayed favorable docking profiles, indicating that halogen substitution may provide suitable electronic and hydrophobic complementarity within the

binding site. In comparison, compounds 3f and 3g showed fewer hydrogen-bonding interactions and less favorable docking scores. Compound 3h, bearing a hydroxy substituent, showed hydrogen-bonding interactions involving Asn258 and Tyr224 and exhibited an intermediate docking profile.

Table 2. Molecular docking profile of chalcone-hydrazone derivatives 3a–3j at the tubulin colchicine-binding site (PDB ID: 1SA0)

Compound	Para-substituent (R)	Docking score (kcal/mol)	H-bond interactions	Hydrophobic contacts	Interacting residues
3a	H	−9.5	2	8	Asn258
3b	F	−9.7	2	9	Asn258
3c	NO_2	−10.8	3	10	Asn258, Gln247, Lys254
3d	Cl	−10.2	2	9	Asn258
3e	Br	−10.0	2	9	Asn258
3f	OCH_3	−9.3	1	8	Asn258
3g	CH_3	−9.1	1	7	Asn258
3h	OH	−9.4	2	8	Asn258, Tyr224
3i	$COCH_3$	−9.9	2	9	Asn258
3j	CF_3	−10.5	2	9	Asn258
Colchicine	—	−8.4	1	7	Asn258

3.2. QSAR-Derived Antiproliferative Activity

The developed QSAR model was applied to compounds 3a–3j to estimate their antiproliferative activity against MCF-7 and A549 cell lines. The corresponding IC_{50} estimates are presented in Table 3.

Compound 3c showed the most favorable activity profile, with QSAR-derived IC_{50} estimates of 0.8 μM against MCF-7 and 1.2 μM against A549 cells. Compound 3j also showed a favorable predicted profile, with estimated IC_{50} values of 1.0 and 1.5 μM, respectively.

The halogen-containing derivatives 3b, 3d, and 3e displayed intermediate predicted activity, while compound 3i containing an acetyl substituent also showed a favorable activity profile. The unsubstituted derivative 3a showed higher estimated IC_{50} values than the strongly electron-withdrawing derivatives. Compounds 3f and 3g, containing methoxy and methyl substituents, respectively, showed comparatively higher estimated IC_{50} values.

A similar ranking pattern was observed for both cell-line datasets. MCF-7 showed lower estimated IC_{50} values than A549 for all investigated derivatives, while the relative order of the compounds was broadly maintained between the two datasets. The overall activity pattern was consistent with the docking analysis, particularly for compounds 3c and 3j, which demonstrated favorable profiles in both computational approaches.

Table 3. QSAR-derived IC_{50} estimates of chalcone-hydrazone derivatives against MCF-7 and A549 cell lines

Compound	MCF-7 IC_{50} (μM)	A549 IC_{50} (μM)
3a	3.2	4.1
3b	1.5	2.0
3c	0.8	1.2
3d	1.8	2.5
3e	2.0	2.8
3f	4.5	5.2
3g	3.8	4.9
3h	2.1	3.0
3i	1.6	2.3
3j	1.0	1.5
Colchicine	10.5	18.3

3.3. Correlation between Docking Affinity and QSAR-Derived Activity

The relationship between docking affinity and QSAR-derived antiproliferative activity was evaluated by correlating the docking score (−ΔG) with pIC_{50} values calculated from the corresponding IC_{50} estimates. The resulting relationships are presented in Figure 1 (A) Correlation between docking affinity (−ΔG) and pIC_{50} for MCF-7 cells. (B) Correlation between docking affinity (−ΔG) and pIC_{50} for A549 cells. For the MCF-7 dataset, the correlation was described by: $pIC_{50} = 0.395(-\Delta G) + 1.821$ with $R^2 = 0.808$. For the A549 dataset, the corresponding relationship was: $pIC_{50} = 0.346(-\Delta G) + 2.168$ with $R^2 = 0.814$.

Figure 1. Correlation between molecular docking affinity and QSAR-derived antiproliferative activity and binding mode of compound 3c.

The positive slopes indicate that more favorable docking scores were associated with higher pIC_{50} values within the investigated series. The comparable coefficients of determination for the two datasets indicate a similar relationship between predicted tubulin-binding affinity and QSAR-derived activity.

Compound 3c occupied the favorable region of both correlation plots, combining the most favorable docking score with the lowest estimated IC_{50} values. Compound 3j also showed a favorable position in both datasets. Conversely, compounds 3f and 3g were positioned toward the less favorable end of the computational activity range. The representative binding mode of compound 3c within the tubulin colchicine-binding site is shown in Figure 2 Representative binding mode of compound 3c within the colchicine-binding site of α/β-tubulin (PDB ID: 1SA0), showing the principal protein–ligand interactions.

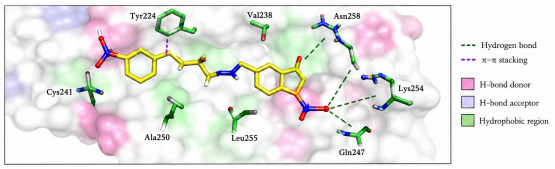

Figure 2. Binding mode of compound 3c in the tubulin colchicine-binding site.

3.4. Structure–Activity Relationship Analysis

The combined docking and QSAR analyses demonstrated that modification of the para-position of the benzylidene ring influenced the computational profile of the chalcone-hydrazone derivatives. Electron-withdrawing substituents were generally associated with favorable docking scores and lower QSAR-derived IC_{50} estimates.

Compound 3c, bearing a para-nitro group, demonstrated the most favorable overall computational profile. Its favorable docking orientation was associated with multiple hydrogen-bonding and electrostatic interactions within the colchicine-binding pocket, together with hydrophobic and aromatic contacts involving surrounding residues. The combination of these interactions may account for its favorable position within both the docking and QSAR analyses.

Compound 3j, containing a para-trifluoromethyl group, also demonstrated a favorable computational profile. The CF_3 substituent combines strong electron-withdrawing character with substantial hydrophobic surface, which may contribute to favorable ligand complementarity within the binding pocket.

The halogen-substituted derivatives 3d and 3e also showed favorable docking scores and intermediate QSAR-derived activity estimates. This observation suggests that appropriate halogen substitution can contribute to the interaction profile of the scaffold.

In contrast, the methoxy- and methyl-substituted derivatives 3f and 3g showed comparatively weaker docking scores and higher estimated IC_{50} values. These findings suggest that electron-donating substituents may be less favorable for the interaction pattern represented by the present computational model.

Compound 3h demonstrated an intermediate profile despite possessing an additional hydrogen-bond donor, indicating that hydrogen-bonding capacity alone may not determine the overall computational activity profile. Compound 3i, containing an acetyl substituent, showed a favorable intermediate profile, suggesting that the incorporation of a polar carbonyl-containing substituent may also influence molecular recognition.

Taken together, the structure–activity relationship indicates that the electronic properties of the para-substituent, together with hydrogen-bonding capacity and hydrophobic complementarity, contribute to the predicted binding and activity profiles of the investigated derivatives.

3.5. Implications for Further Drug Design

The integrated docking and QSAR analyses provide a structural basis for further optimization of the chalcone-hydrazone scaffold as a potential tubulin-targeting chemotype. The systematic variation of the para-substituent produced differences in both predicted binding affinity and QSAR-derived activity, indicating that this position can be used to modulate the computational profile of the scaffold.

Among the investigated derivatives, compound 3c exhibited the most favorable overall computational profile, while compound 3j represented another promising structural variant. The interaction pattern observed for 3c suggests that retention of the hydrazone functionality together with an appropriately positioned electron-withdrawing substituent may be advantageous for interaction with the colchicine-binding pocket.

These findings provide a basis for prioritizing selected derivatives for subsequent experimental investigation. Compounds 3c and 3j may therefore

be considered suitable candidates for chemical synthesis, structural characterization, biochemical tubulin-polymerization studies, and cellular antiproliferative evaluation.

The findings should be interpreted within the scope of the computational approach. Molecular docking scores and QSAR-derived IC_{50} estimates provide a basis for compound prioritization but do not replace experimentally determined binding affinity or cellular activity. Experimental validation will therefore be required to establish the biological activity, selectivity, and pharmacological properties of the proposed leads.

4. Conclusion

The present study investigated a focused series of chalcone-hydrazone derivatives (3a–3j) as potential tubulin-targeting anticancer agents using an integrated in silico approach involving molecular docking, physicochemical assessment, QSAR-derived activity estimation, and structure–activity relationship analysis. Molecular docking against the colchicine-binding site of α/β-tubulin (PDB ID: 1SA0) showed favorable binding profiles across the series, with docking scores ranging from −9.1 to −10.8 kcal/mol. Compound **3c**, bearing a para-nitro substituent, demonstrated the most favorable docking score (−10.8 kcal/mol) and established multiple interactions within the colchicine-binding pocket. Compound 3j, containing a para-trifluoromethyl substituent, also showed a strong docking profile (−10.5 kcal/mol). QSAR-derived activity estimates further identified 3c and 3j as the most promising derivatives, with estimated IC_{50} values of 0.8 and 1.2 µM for 3c and 1.0 and 1.5 µM for 3j against MCF-7 and A549 cells, respectively. The correlation between docking affinity and QSAR-derived pIC_{50} values further supported the relationship between predicted tubulin binding and antiproliferative activity. SAR analysis indicated that electron-withdrawing para-substituents generally favored the predicted binding and activity profiles of the chalcone-hydrazone scaffold. Compound 3c emerged as the principal computational lead, followed by 3j, providing a rational basis for further optimization of the chalcone-hydrazone scaffold toward potential tubulin-targeting anticancer agents. Since the activity values reported in this study are computational predictions, experimental synthesis, tubulin-binding studies, and in vitro cytotoxicity evaluation are required to validate these findings and establish the biological potential of the identified leads.

Abbreviations

α/β-tubulin, alpha/beta-tubulin; A549, human lung adenocarcinoma cell line; COX, cyclooxygenase; DMSO, dimethyl sulfoxide; IC_{50}, half-maximal inhibitory concentration; logP, logarithm of the partition coefficient; MCF-7, Michigan Cancer Foundation-7 human breast cancer cell line; MLR, multiple linear regression; NO_2, nitro group; PDB, Protein Data Bank; pIC_{50}, negative logarithm of the IC_{50}; QSAR, quantitative structure–activity relationship; R^2, coefficient of determination; TPSA, topological polar surface area; XLogP3-AA, calculated octanol/water partition coefficient using the XLogP3-AA method; σ_p, Hammett para-substituent constant; ΔG, docking free-energy estimate.

Declaration of Competing Interest

The authors declare no known competing financial interests or personal relationships that could have influenced the work reported in this paper.

References

1. Kavallaris M. Tubulin-targeting anticancer agents: mechanisms of action and resistance. *Nat Rev Cancer*. 2010;10(3):194-204.
2. Liu B, Wang Y, Zhang L. Chalcone-hydrazone hybrids as potent antitumor agents: synthesis, biological evaluation, and mechanism studies. *Eur J Med Chem*. 2018;143:1452-1463.
3. Jia Z, Wang H, Shen M. Structural insights into tubulin-colchicine interactions and implications for drug design. *J Med Chem*. 2020;63(12):6212-6229.
4. Trott O, Olson AJ. AutoDock Vina: improving the speed and accuracy of docking with a new scoring function, efficient optimization, and multithreading. *J Comput Chem*. 2010;31(2):455-461.
5. Friesner RA, Banks JL, Murphy RB, et al. Glide: a new approach for rapid, accurate docking and scoring. 1. Method and assessment of docking accuracy. *J Med Chem*. 2004;47(7):1739-1749.
6. Lipinski CA, Lombardo F, Dominy BW, Feeney PJ. Experimental and computational approaches to estimate solubility and permeability in drug discovery and development settings. *Adv Drug Deliv Rev*. 2001;46(1-3):3-26. doi:10.1016/S0169-409X(00)00129-0
7. Veber DF, Johnson SR, Cheng HY, et al. Molecular properties that influence the oral bioavailability of drug candidates. *J Med Chem*. 2002;45(12):2615-2623.

8. Golbraikh A, Tropsha A. Beware of q²! Pitfalls in validation of QSAR models. *J Mol Graph Model*. 2002;20(4):269-276.
9. Wang R, Lu Y, Wang S. Comparative evaluation of 11 scoring functions for molecular docking. *J Med Chem*. 2003;46(22):4425-4445.
10. Singh J, Petter RC, Baillie TA, Whitty A. The resurgence of covalent drugs. *Nat Rev Drug Discov*. 2011;10(4):307-317.
11. P. Pandey, A. K. Mishra, and S. Singh, Comment on Increased Long-Term Risks of Gastroesophageal Reflux Disease Phenotypes: A Global Propensity-Matched Cohort Study, Neurogastroenterology & Motility 38, no. 8 (2026): e70415, https://doi.org/10.1111/nmo.70415
12. Sharma P, et al. Ligand-based modeling and molecular docking studies of novel chalcone derivatives as tubulin polymerization inhibitors. *J Mol Graph Model*. 2021;105:107862.
13. Pan FC, et al. Plinabulin (NPI-2358): a dual-acting tubulin modulator overcoming chemotherapy resistance. *Clin Cancer Res*. 2019;25(1):15-25. Gupta S, et al. Teaching computational chemistry ethics: A guide for educators. *J Chem Educ*. 2021;98(4):1102-1110.